

図1 ハット積層型カーボンナノファイバー(H-CNFs) (Yokoyama A et al., 2005¹⁵⁾より一部改変
 a: H-CNFs 模式図. b: SEM像. c: TEM像. 矢印: グラフェンエッジ. d: cの拡大像. e: EDX分析

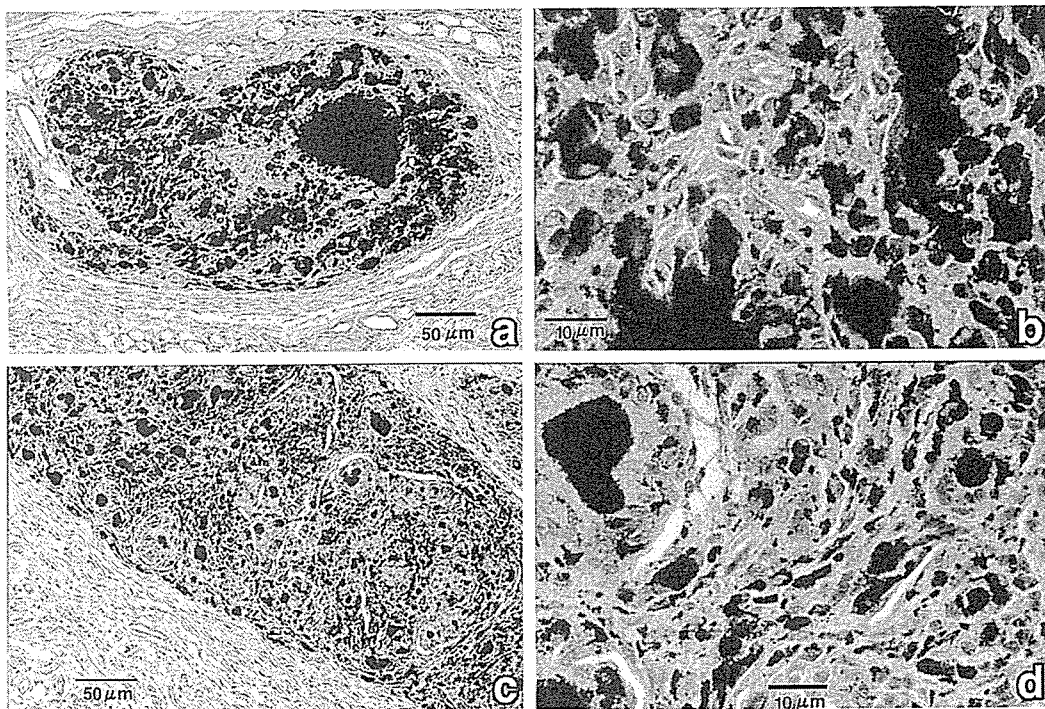


図2 H-CNFs皮下埋入後の組織像(Yokoyama A et al., 2005)¹⁵⁾
 a: 埋入1週後. b: aの拡大像. c: 埋入4週後. d: cの拡大像

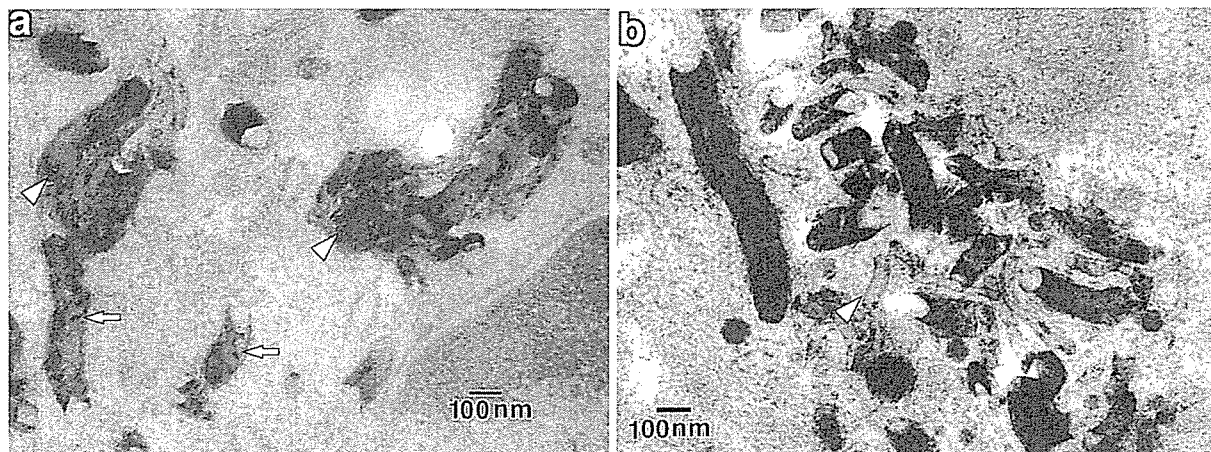


図3 H-CNFs皮下埋入後のTEM像
(Yokoyama A et al., 2005)¹³⁾

a: 埋入1週後. 矢印: H-CNFs. 矢頭: 凝集したH-CNFs
b: 埋入4週後. 矢頭: 半透明化したH-CNFs

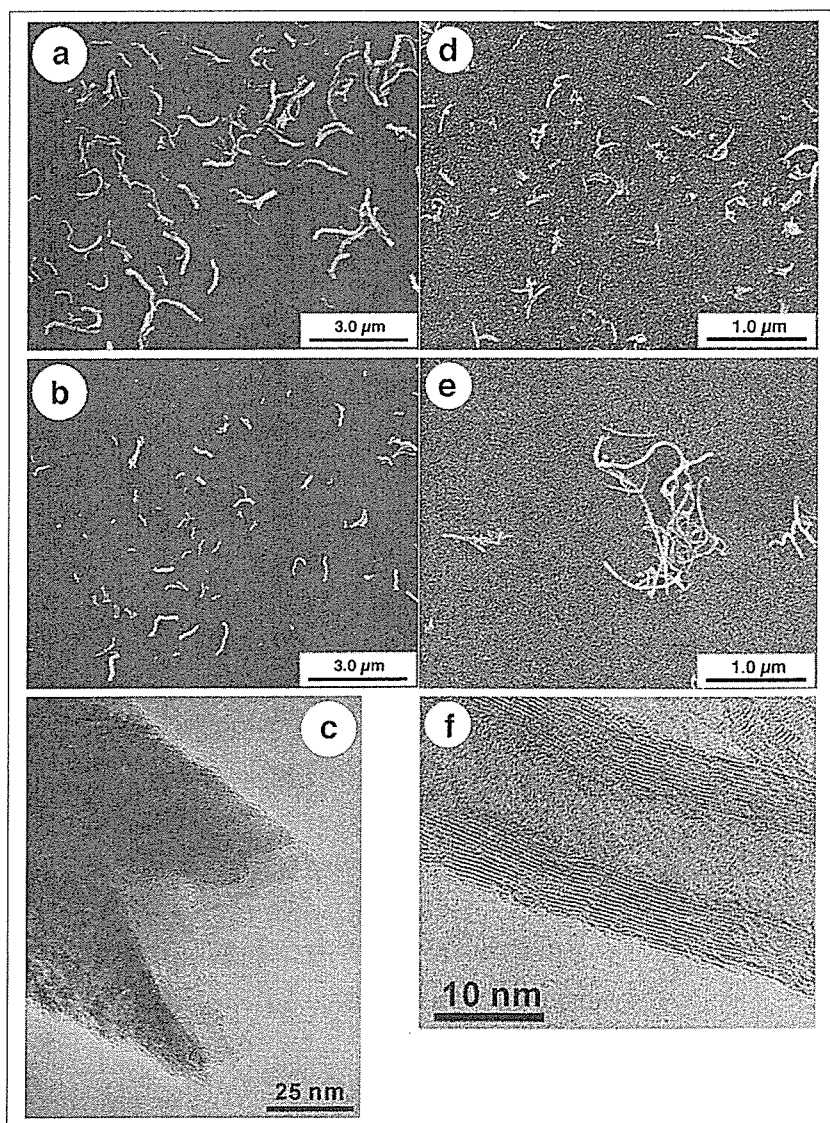


図4
サイズを制御したH-CNFsとMWCNTs
a: 1200H-CNFs SEM像
b: 600H-CNFs SEM像
c: H-CNFs TEM像
d: 220MWCNTs SEM像
e: 825MWCNTs SEM像
f: MWCNTs TEM像

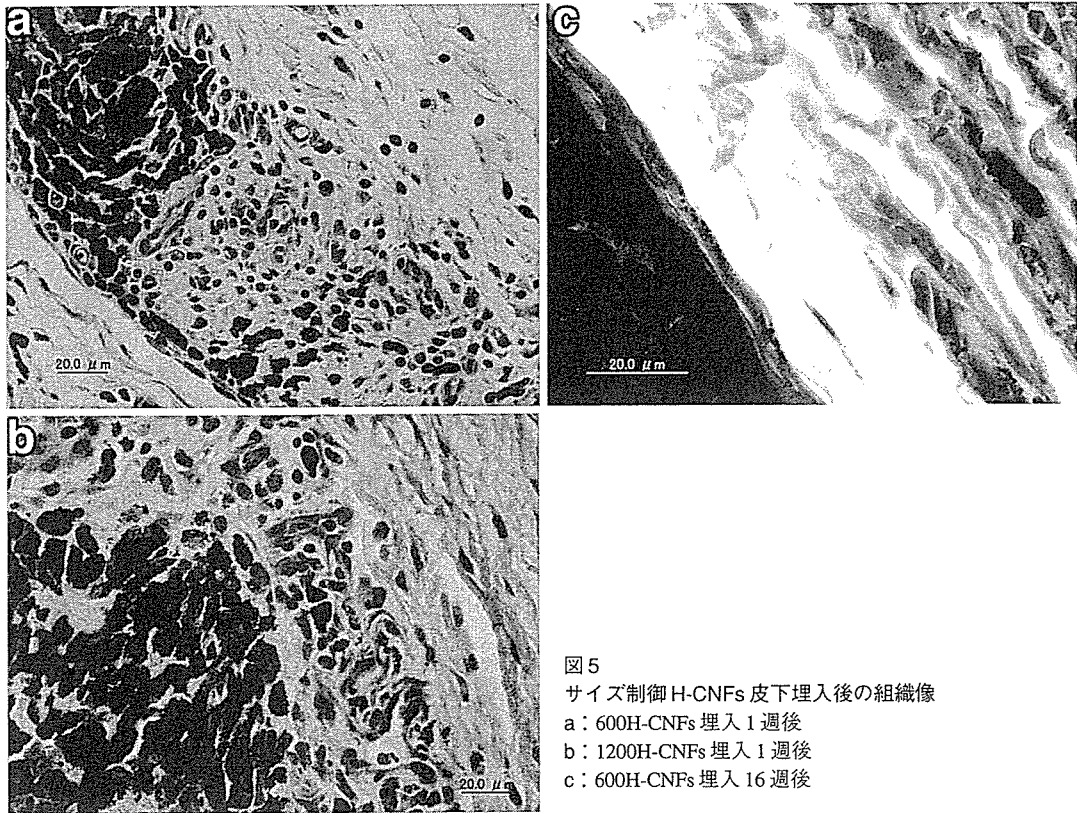


図5
 サイズ制御 H-CNFs 皮下埋入後の組織像
 a: 600H-CNFs 埋入 1 週後
 b: 1200H-CNFs 埋入 1 週後
 c: 600H-CNFs 埋入 16 週後

り、精製されたカーボンナノ物質としてハット積層型カーボンナノファイバー (hat stacked carbon nanofibers: H-CNFs) の供与を受け、予備実験的に埋入試験を行った。

H-CNFsの生体内挙動

1. H-CNFs

H-CNFsは、化学気相蒸着 (CVD) により Ni 触媒を用いて合成され、傘状のグラフェンシートが面間隔約 0.34 nm で積層された形態をしている²⁰⁾ (図1)。

2. 埋入試験

長さ 0.1 ~ 1 μm、直径 30 ~ 100 nm の H-CNFs を、6 週齢オス、ウイスターラットの胸部皮下組織に埋入した。1 および 4 週で灌流固定後、周囲組織とともに H-CNFs を摘出し、浸漬固定を行った。通法に従いパラフィン包埋を行い、薄切後、ヘマトキシリン-エオジン染色を行い光学顕微鏡にて観察した。一部の試料については、Epon812 に包埋後、約 80 nm の超薄切片を作製し、酢酸ウラニルと硝酸鉛による

重染色後、透過型電子顕微鏡 (TEM) による観察を行った。

3. H-CNFs に対する反応

埋入 1 週後、H-CNFs 集塊は、比較的薄い線維性結合組織の被膜で覆われており、H-CNFs 粒子周囲には多数のマクロファージや異物巨細胞が認められた。これらの貪食系細胞の細胞質内にも、H-CNFs の小さな粒子が観察された (図2a, b)。4 週後においても H-CNFs 粒子周囲には、間葉系の細胞や異物巨細胞が多数観察され、いわゆる肉芽腫性炎の状態を呈していたが、壊死や好中球の浸潤などの強い炎症反応は観察されなかった (図2c, d)。TEM 観察において、1 週後にマクロファージや異物巨細胞内に多数の貪食された H-CNFs 粒子が観察された。H-CNFs の多くは、互いに凝集し、膜に覆われてライソゾーム内に認められたが、一部に膜構造が観察されないものも認められた (図3)。これらの結果から、H-CNFs の起炎性は強くないこと、マクロファージに貪食されることが明らかとなった¹⁵⁾。

細胞内で H-CNFs の長さの短縮や構造の変化を

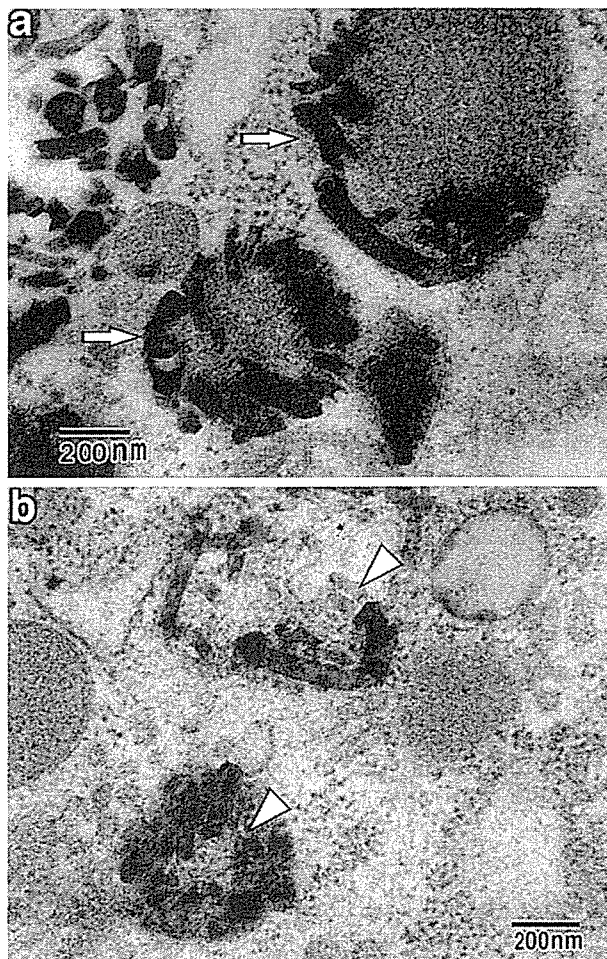


図6 600H-CNFs皮下埋入後のTEM像
 a: 埋入1週後. 矢印: H-CNFsを取り込んだライソソーム
 b: 埋入16週後. 矢頭: 短縮や半透明化したH-CNFs

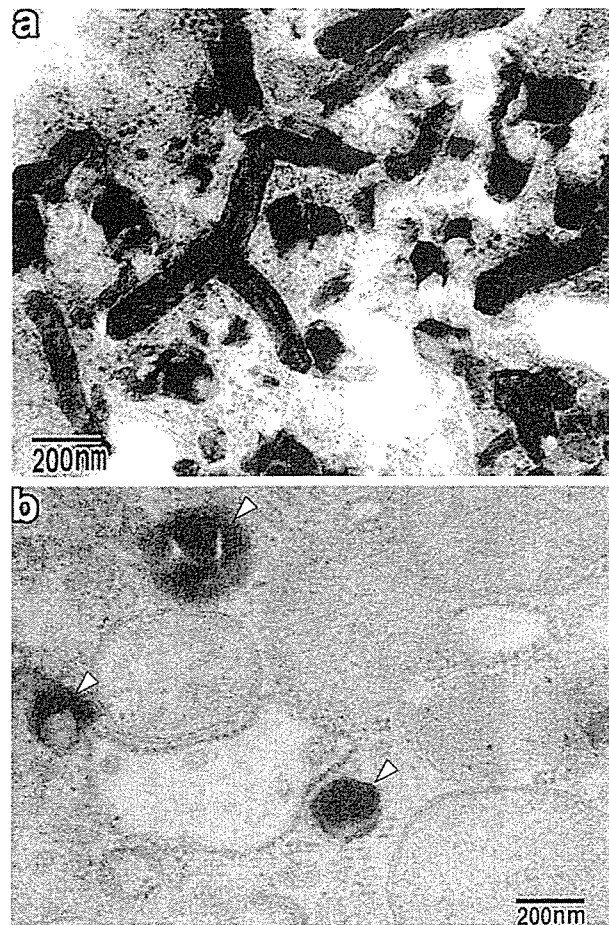


図7 1200H-CNFs皮下埋入後のTEM像
 a: 埋入1週後
 b: 埋入16週後. 矢頭: 短縮し、構造が変化したと推察されるH-CNFs

示唆する所見も認められたが、埋入したH-CNFsの長さにはばらつきがあることから、長さを制御するとともに、同じカーボンナノ物質でもグラフェンシートが継ぎ目のない状態でチューブ状を呈する構造がまったく異なる多層カーボンナノチューブ(MWCNTs)と比較するため、以下の研究を行った。

カーボンナノ物質のサイズと構造が細胞内挙動に及ぼす影響

1. 試料

精製しサイズを制御したH-CNFsとMWCNTsは、東北大学大学院環境科学研究科の田路研究室より供与を受けた。

(1) サイズ制御 H-CNFs

長さの制御は、濃硫酸(95%)：濃硝酸(60%) = 3：1(v/v%)の混合液に入れ、超音波照射により行った。洗浄、濾過後、さらにエタノール中で1時間超音波処理を行い、直径2.0、1.2、および0.4 μmの濾過膜で順に濾過し、平均長さ590 nmと1,160 nmのH-CNFsを得た(以下、600 H-CNFsおよび1200 H-CNFsとする)(図4a～c)。

(2) サイズ制御 MWCNTs

原材料としてNano Lab社製のMWCNTsを用いた。触媒を除去するため、塩酸および水酸化ナトリウムで洗浄後、95%硫酸と60%硝酸を3：1で混合した溶液中で5時間超音波処理を行い、MWCNTsを精製した。得られたMWCNTsの長さを制御するため、エタノール中で1時間超音波処理し、ポリカー

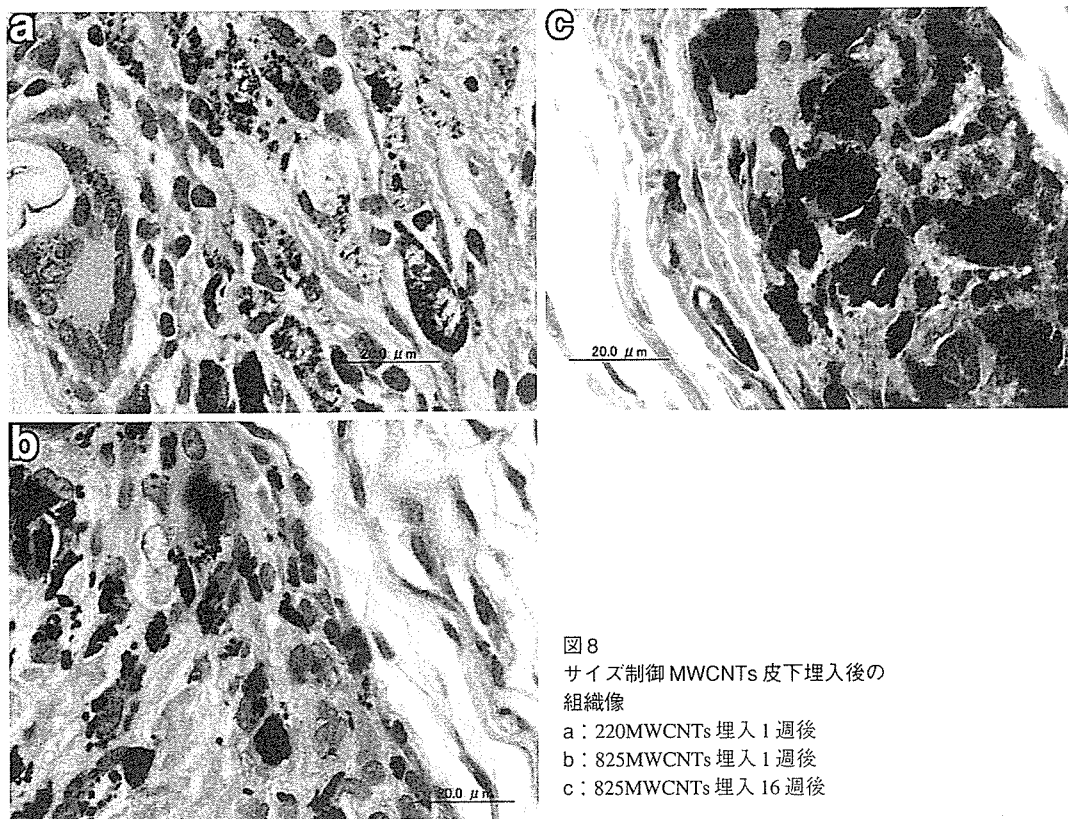


図8
サイズ制御MWCNTs皮下埋入後の
組織像
a: 220MWCNTs埋入1週後
b: 825MWCNTs埋入1週後
c: 825MWCNTs埋入16週後

ポネート製の直径2.0, 1.2, 0.8, および0.4 μm の濾過膜で順に濾過し, 平均長さ220 nmおよび825 nmのMWCNTsを得た¹⁸⁾(以下, 220 MWCNTsおよび825 MWCNTsとする. 精製およびサイズ制御の詳細については田路・佐藤論文を参照されたい)(図4 d~f).

2. カーボンナノ物質に対する反応

皮下組織への埋入試験は, 長さ未制御のH-CNFsと同様に行ったが, 観察期間は16週まで行った.

(1) H-CNFs

埋入1週後では, 大きな塊状の600 H-CNFsは, 線維性結合組織に被包されていたが, 多くの600 H-CNFsはマクロファージや線維芽細胞に貪食されており, 炎症は軽微であった(図5a). 16週後では, 600 H-CNFsを貪食したマクロファージの集積が観察され, 薄い線維性結合組織被膜に覆われていた. 線維芽細胞内およびコラーゲン線維に沈着しているCNFsも観察された(図5c). TEM観察では, 1週後, 多くの600 H-CNFsは細胞質内で円形に集合しており, ライソゾーム内にも600 H-CNFsが観察された

(図6a). 16週後においては, ほとんどの600 H-CNFsは, ライソゾーム中に認められた. ライソゾーム中の600 H-CNFsには, 長さの短縮, および半透明化などの結晶構造の変化を示唆する像も観察された(図6b).

1200 H-CNFsは, 1週後では, 600 H-CNFsと同様にマクロファージや線維芽細胞に貪食されているものが多数認められたが, 貪食されていないものが600 H-CNFsに比較し多く観察された. 炎症は軽微であるが, 600 H-CNFsに比較しやや強い傾向を示した(図5b). 16週後においては, 600 H-CNFsとはほぼ同様の所見を呈していた. TEM観察においては, 1週では, 細胞質内に1200-CNFsが多数観察されたが, ライソゾーム内には認められなかった(図7a). 16週では, 細胞質内に円形に集合している1200 H-CNFsが多数認められ, 一部のものはライソゾーム内に存在し, 600 H-CNFsと同様に, 短縮や結晶構造の変化を示唆する像が観察された(図7b).

(2) MWCNTs

220 MWCNTsの多くは, 埋入1週後において, マクロファージや線維芽細胞内に観察され, 大きな集

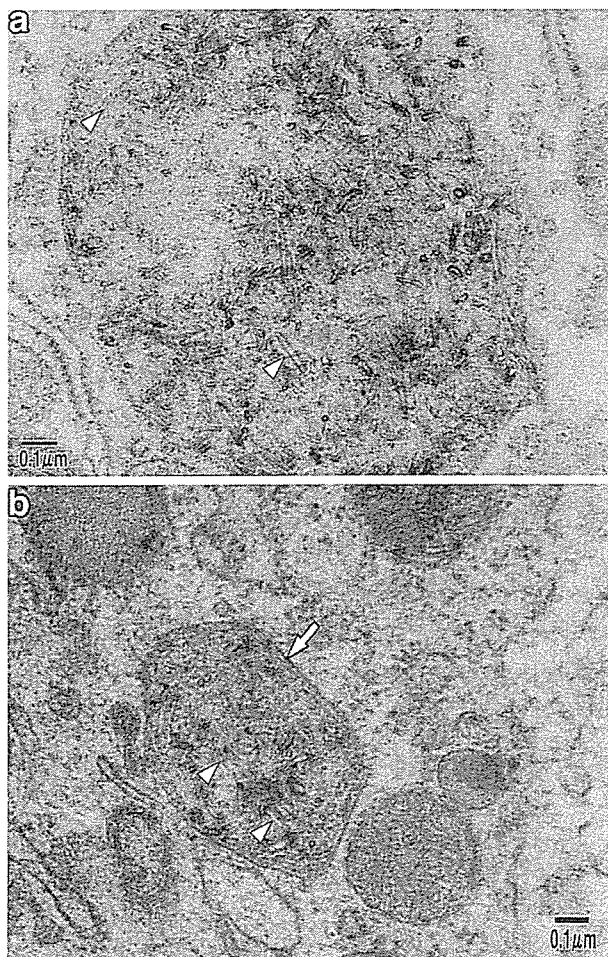


図9 220MWCNTs皮下組織埋入後のTEM像

- a: 埋入1週後. 矢頭: ライソゾーム中のMWCNTs
 b: 埋入16週後. 矢印: MWCNTsを取り込んだライソゾーム. 矢頭: ライソゾーム中のMWCNTs

塊周囲には異物巨細胞が観察されたが、変性や壊死といった強い炎症反応は観察されなかった(図8a)。16週においては、220 MWCNTsはマクロファージやコラーゲン線維間の線維芽細胞中に観察された。比較的大きな集塊の周囲には異物巨細胞が観察されたが、強い炎症反応は認められなかった。TEM観察において、1週では、220 MWCNTsの多くは、マクロファージ中のライソゾーム内に観察された。220 MWCNTsは凝集しており、特有なチューブ状の形態には変化は認められなかった(図9a)。16週では、1および4週同様に220 MWCNTsは、マクロファージや線維芽細胞内のライソゾーム中に観察された。その多くは凝集しており、チューブ状の形態に変化は認められなかった(図9b)。

埋入1週後、825 MWCNTs周囲には肉芽組織が

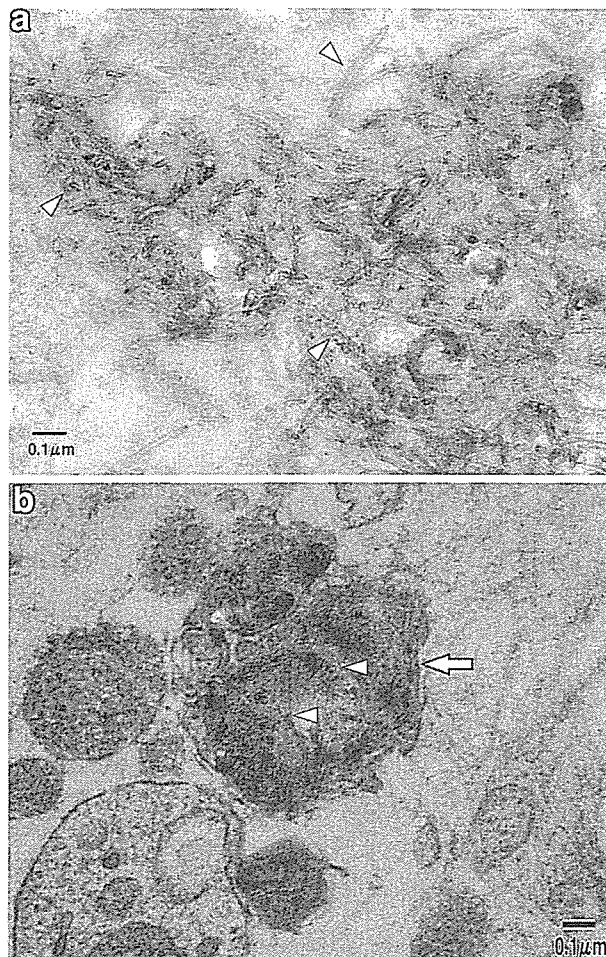


図10 825MWCNTs皮下組織埋入後のTEM像

- a: 埋入1週後. 矢頭: 細胞質中のMWCNTs
 b: 埋入16週後. 矢印: MWCNTsを取り込んだライソゾーム. 矢頭: MWCNTs

観察された。220 MWCNTsと比較すると炎症反応はやや強い傾向を示した。825 MWCNTsの一部は、マクロファージに貪食されていた(図8b)。埋入16週後では、825 MWCNTsの多くは、マクロファージや線維芽細胞内に観察されたが、一部の825 MWCNTsの集塊周囲に異物巨細胞が多数認められ、肉芽腫性炎を呈していた(図8c)。TEMにおいては、1週では、細胞間に多数の825 MWCNTsが観察されたが、マクロファージの細胞質内にも凝集したCNTsが認められ、膜構造で覆われていないものが多かった(図10a)。16週では、ライソゾームに存在する825 MWCNTsが多く認められるようになったが、そのチューブ状の構造に変化は観察されなかった(図10b)。

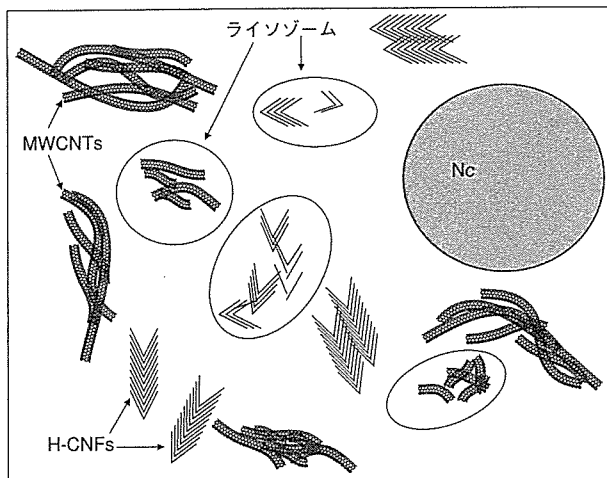


図11 カーボンナノ物質の細胞内での挙動の模式図
 サイズの大きいもの、凝集の強いものはライソゾーム内には認められない。MWCNTsの構造は変化が認められないが、H-CNFsには短縮や結晶構造の変化が示唆される。このようにナノ物質のサイズや構造は細胞内挙動に影響する。

3. サイズと構造が起炎性と細胞内挙動に及ぼす影響

CNFsについては、観察した期間中、変性や壊死などの強い炎症反応は認められず、埋入初期に軽微な炎症が認められるにすぎなかった。長さが異なる2種を試料として用いたが、長い1200 H-CNFsの炎症反応のほうが、600 H-CNFsに比較しやや強い傾向を示した。この原因として、1200 H-CNFsのほうがマクロファージに貪食されにくいことが考えられる。これは、TEM 所見からも裏付けられ、600 H-CNFsは、埋入1週においてライソゾーム中に認められるものがあり、多くのH-CNFsが、細胞質内において円形に集合していた。このことから、マクロファージ内でCNFsの処理が1週においてすでに進行していることが推察される。

1200 H-CNFsにおいても、16週後においては、ライソゾーム内に多数のH-CNFsが観察され、経時的にマクロファージ内で1200H-CNFsの処理が進んでいることが示唆された。これには、凝集しているH-CNFsの分散やH-CNFsの切断による短縮が関係するものと考えられる。

ライソゾーム中に観察されるH-CNFsは、いずれの長さのH-CNFsであっても、400 nm以下のものが多かった。短くなったものがライソゾームのなかに入りやすいのか、あるいはライソゾーム内でH-CNFsの切断と短縮が生じるのかは明らかではない

が、H-CNFsは、マクロファージ内で処理される可能性が示唆された。

H-CNFsは、傘状のグラフェンシートが積層された構造をしており、1枚1枚のグラフェンシートはファンデルワールス力で結合しているため、切断には大きなエネルギーを要しない。また、グラフェンシートのエッジには水酸基があり、細胞内の酵素や蛋白と容易に結合することが可能であり、いわゆるデラミネーション²¹⁾が起りやすいこともH-CNFsの切断と短縮に関係するものと考えられる。また、興味深い所見として、埋入16週でライソゾーム内において一部に、H-CNFsの特有の構造である積層された傘状の構造に変化が認められた。これは、グラフェンシートの結晶構造の変化と考えられるが、詳細については今後さらなる研究が必要と考えられる。

細胞内でのH-CNFsの切断と短縮が示唆されたことは、DDSのキャリアとしての可能性を示すものであり、今後、生理活性物質と複合などの研究が期待される。

MWCNTsの起炎性は、H-CNFs同様に長いほうが起炎性は強く、埋入16週においても異物巨細胞が集積するいわゆる肉芽腫性炎が認められた。TEM所見からも、220 MWCNTsが1週後からライソゾーム内に認められるのに対し、825 MWCNTsでは、細胞間に存在するものが多く、細胞内においても細胞質内で凝集して存在しているものが多いことから、長いMWCNTsのほうが、マクロファージで処理されにくいことが示唆された。これは、Sato¹⁸⁾が報告しているように、長いMWCNTsの凝集性のほうが強く、さらに825 MWCNTsは湾曲が強い形であり、凝集した状態から分離しにくいことなどに起因するものと推察された。16週においては、220 MWCNTsに比較するとその数は少ないが、825 MWCNTsにおいても一部のライソゾーム内にMWCNTsが観察された。

これらのことから、MWCNTsは細胞質、ライソゾーム内で蛋白や酵素の影響を受け凝集程度が弱くなったものと考えられた。また、H-CNFsと異なり、MWCNTsでは、切断、短縮や結晶構造の明らかな変化は認められず、チューブ状の構造が埋入16週においても維持されていた。これは、MWCNTsは炭素の六員環が連続している結晶構造をとるため、

機械的強度が強だけでなく、化学的に安定であることも関係すると推察された。起炎性については、MWCNTsのほうがH-CNFsに比較し強い傾向を示したが、このような構造の差に基づく細胞の反応が関係している可能性が示唆された。

カーボンナノ物質に対する生体反応に関しては、冒頭で述べたように最近ようやく研究されるようになってきた。SWCNTsを気管内に強制曝露し、間質性の肉芽腫および壊死を報告したLam¹³⁾は、CNTsの構造と物理化学的な性質によるものではないかと考察している。一方、Koyama¹⁴⁾は、皮下にSWCNTs、MWCNTsなどのカーボンナノ物質を埋入し、アスベストに比較し起炎性が弱いことを報告している。しかし、これらの報告はいずれも光学顕微鏡レベルで観察されたものであり、ナノ物質の細胞内での挙動については、その大きさや構造を考慮するとTEMレベルでの検討も必要と思われる。また、埋入部位や濃度(量)などの条件も、生体反応に大きく関与するため、さらに、詳細かつ総合的な研究が必要であろう。

おわりに

これまでの研究で、同じカーボンナノ物質であっても、その構造や長さにより生体に対する反応および生体内での挙動が異なることが示唆された(図11)。現在、さらに長期埋入について検討を行っており、埋入1年後の結果が出つつある。今後、これらの結果を生体材料の開発に活かすとともに、さらにカーボンナノ物質の体内での動態などの安全性に関する研究を進めていく予定である。

本研究は、厚生科研費(H14-ナノ-021)、文部科学省科研費(16390549)によるものである。

文 献

- 1) Iijima S : Helical microtubules of graphitic carbon. *Nature* 1991, 354 : 56-58.
- 2) Murakami T, Ajima K, Miyawaki J, Yudasaka M, Iijima S, Shiba K : Drug-loaded carbon nanohorns : Adsorption and release of dexamethasone *in vitro*. *Mol Pharm* 2004, 1 : 399-405.
- 3) Isobe H, Nakanishi W, Tomita N, Jinno S, Okayama H, Nakamura

- E : Nonviral gene delivery by tetraamino fullerene. *Mol Pharm* 2006, 3 : 124-134.
- 4) Fugetsu B, Satoh S, Shiba T, Mizutani T, Lin Y et al. : Caged multi-walled carbon nanotubes as the adsorbents for affinity-based elimination of Ionic dyes. *Environmental Science & Technology* 2004, 38 : 6890-6896.
- 5) Aoki N, Yokoyama A, Nodasaka Y, Akasaka T, Uo M et al. : Cell culture on a carbon nanotube scaffold. *J of Biomed Nanotech* 2005, 1 : 402-405.
- 6) Aoki N, Yokoyama A, Nodasaka Y, Akasaka T, Uo M et al. : Strikingly extended morphology of cells grown on carbon nanotubes. *Chem Lett* 2006, 35 : 508-509.
- 7) Schvedova AA, Castranova V, Kisin ER, Schwegler-Berry D, Murray AR et al. : Exposure to carbon nanotube material : assessment of nanotube cytotoxicity using human keratinocyte cells. *J Toxicol Environ Health A* 2003, 21 : 1166-1170.
- 8) Monteiro-Riviere NA, Nemanich RJ, Inman AO, Wang YY, Riviere JE : Multi-walled carbon nanotubes interactions with human epidermal keratinocytes. *Toxicol Lett* 2005, 155 : 377-384.
- 9) Kirchner C, Liedl T, Kudera S, Pellegrino T, Javier AM et al. : Cytotoxicity of colloidal CdSe and CdSe/ZnS nanoparticles. *Nano Lett* 2005, 5 : 331-338.
- 10) Huczko A, Lange H : Carbon nanotubes : experimental evidence for a null risk of skin irritation and allergy. *Fullerene Sci Technol* 2001, 9 : 247-250.
- 11) Huczko A, Lange H, Calko E, Grubek-Jaworska H, Droszcz P : Physiological testing of carbon nanotubes : are they asbestos-like? *Fullerene Sci Technol* 2001, 9 : 251-254.
- 12) Warheit DB, Laurence BR, Reed KL, Roach DH, Reynolds GAM, Webb TR : Comparative pulmonary toxicity assessment of single-wall carbon nanotubes in rats. *Toxicol Sci* 2004, 77 : 117-125.
- 13) Lam CW, James JT, McCluskey R, Hunter RL : Pulmonary toxicity of single-wall carbon nanotubes in mice 7 and 90 days after intratracheal instillation. *Toxicol Sci* 2004, 77 : 126-134.
- 14) Koyama S, Endo M, Kim YA, Hayashi T, Yanagisawa T et al. : Roll of systemic T-cells and histopathological aspects after subcutaneous implantation of various carbon nanotubes in mice. *Carbon* 2006, 44 : 1079-1092.
- 15) Yokoyama A, Sato Y, Nodasaka Y, Yamamoto S, Kawasaki T et al. : Biological behavior of hat-stacked carbon nanofibers in the subcutaneous tissue in rats. *Nano Lett* 2005, 5 : 157-161.
- 16) Uo M, Tamura K, Sato Y, Yokoyama A, Watari F et al. : The cytotoxicity of metal-encapsulating carbon nanocapsules. *Small* 2005, 1 : 816-819.
- 17) Sato Y, Shibata K, Kataoka H, Ogino S, Fugetsu B et al. : Strict preparation and evaluation of water-soluble hat-stacked carbon nanofibers for biomedical application and their high biocompatibility : influence of nanofiber-surface functional groups on cytotoxicity. *Molecular BioSystems* 2005, 1 : 142-145.
- 18) Sato Y, Yokoyama A, Shibata K, Akimoto Y, Nodasaka Y et al. : Influence of length on biocompatibility of multi-walled carbon nanotubes by human acute monocytic leukemia cell line THP-1 *in vitro* and subcutaneous tissue of rats *in vivo*. *Molecular BioSystems* 2005, 1 : 176-182.
- 19) Yokoyama A, Sato Y, Nodasaka Y, Yamamoto S, Aoki N et al. : Tissue response to carbon nanosubstances : comparison between carbon nanotubes and hat-stacked carbon nanofibers by transmission electron microscopy. *Extended Abstracts ISETS05* 2005, 625-628.
- 20) Sato Y, Jeyadevan B, Tohji K, Tamura K, Akasaka T et al. : Water-soluble hat-stacked-type carbon nanofibers for biomedical applications. Abstract No 1625. 206th Meeting of ECS, 2004.
- 21) Liu Z, Ooi K, Kanoh H, Tang W, Tomida T : Swelling and delamination behaviors of birnessite-type manganese oxide by intercalation of tetraalkylammonium ions. *Langmuir* 2000, 16 : 4154-4164.

Strikingly Extended Morphology of Cells Grown on Carbon Nanotubes

Naofumi Aoki,^{*1} Atsuro Yokoyama,¹ Yoshinobu Nodasaka,¹ Tsukasa Akasaka,¹ Motohiro Uo,¹
Yoshinori Sato,² Kazuyuki Tohji,² and Fumio Watari¹

¹Graduate School of Dental Medicine, Hokkaido University, Kita 13, Nishi 7, Kita-ku, Sapporo 060-8586

²Graduate School of Environmental Studies, Tohoku University, Sendai 980-8576

(Received February 7, 2006; CL-060164; E-mail: nao11@den.hokudai.ac.jp)

The morphology of cells cultured on carbon nanotube (CNTs) scaffolds was investigated using a confocal laser scanning microscope (CLSM) and a scanning electron microscope (SEM) and it was shown that the cells extended strikingly in all directions and numerous filopodia extended far from the cells.

Carbon nanotubes (CNTs) have attracted great interest since their discovery was reported by Iijima in 1991 because of their unique structure-dependent electrical and mechanical properties.¹ However, there have been very few studies on their biomedical application.^{2,3} Some reports suggest the possible toxicity of CNTs.⁴ In contrast, our recent studies employing *in vitro* and *in vivo* experiments showed their excellent properties as scaffolds for cell culture.^{5,6} Cell morphology and proliferation have been investigated in *in vitro* studies, most of which were performed using nerve cells.⁷ CNTs support nerve cell functions and growth, and our previous studies showed that the cells on CNTs grew well.⁵ Thus, further investigation of interactions between CNTs and cells was deemed necessary to evaluate their biocompatibility and develop biological applications. There are only a few reports about the morphology of osteoblasts on CNTs.⁸ The present study reports observations on the relationship between cells and CNTs and quantitative analysis of the morphology of osteoblasts grown on CNTs examined via scanning electron microscopy and confocal laser scanning microscopy, respectively.

CNTs 5–20 nm in diameter and 20–40 μm in length synthesized by chemical vapor deposition (NanoLab, Inc. MA, U.S.A.) were treated with hydrochloric acid to remove the metal catalyst. The purity was about 98 wt %.⁹ CNTs (200 μg) were dispersed in 100 mL of deionized water by sonication for 3 min. CNT scaffolds were made by vacuum filtration of the dispersed CNT slurry onto porous polycarbonate membranes (PC; 47 mm diameter and 0.8 μm pore size, ADVANTEC, Japan). After drying for 3 h at 60 $^{\circ}\text{C}$, CNTs were fixed on membranes, and coated and non-coated membranes were placed in polystyrene dishes 60 mm in diameter and sterilized under UV light for 24 h. Then, 1.0×10^5 human osteoblast-like cells (SaOS2 cells) were seeded onto each scaffold (PC and CNTs) and cultured in Dulbecco's modified Eagle's medium (DMEM; SIGMA) with 10% fetal bovine serum (FBS; Biowest) and 1% penicillin/streptomycin under standard cell culture conditions (at 37 $^{\circ}\text{C}$ in a humidified 5% CO_2 /95% air environment) for 7 days. After cell culture for 7 days, the samples were washed with PBS to remove nonadherent cells on the scaffolds and fixed with a solution of 2% glutaraldehyde, and post-fixed in 1% osmium tetroxide. Then, the samples were dehydrated in graded series of alcohol (50, 70, 80, 90, 95, and 100%) and isoamyl acetate following critical-point drying. The cell morphology was observed and profiled using a confocal

laser scanning microscope (CLSM; VK-9500, KEYENCE, Japan). A scanning electron microscope (SEM; S4000, Hitachi, Japan) was used for investigation of the peripheral parts of SaOS2 cells grown on CNTs.

Figure 1 shows the CLSM images demonstrating the morphology of SaOS2 cells cultured for 7 days on PC and CNTs. Note the difference of the scale bars. Cells on PC were elongated in one direction (Figure 1a), whereas there was excellent proliferation with extension of cells in all directions on CNTs (Figure 1b). The cells on CNTs were about 10 times larger than those on PC. Figure 2 shows a comparison of the cross-section profiles of from the different cultures. The length and the height of the cell were 12.13 and 6.83 μm on PC, and 113.14 and 4.35 μm on CNTs, respectively. The contact angle for the cell and substrate was much smaller on CNTs (4.4 $^{\circ}$) than that on PC (28.3 $^{\circ}$). The cells on CNTs were wider and flatter than those on PC.

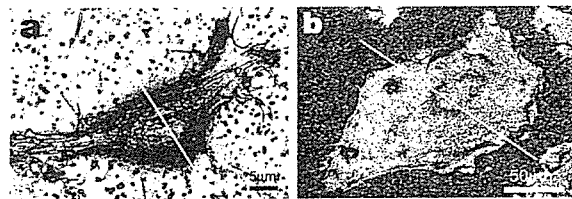


Figure 1. Cell morphology from culture on PC (a) and CNTs (b) observed by a confocal laser scanning microscope (CLSM). Note the difference of scale bars. Cells were fully developed on CNTs. The line show cross section referred to in Figure 2.

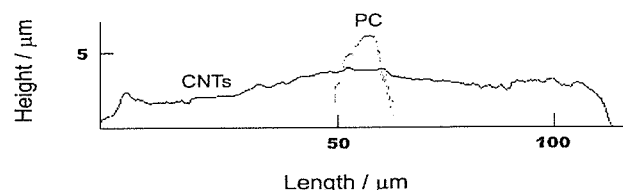


Figure 2. Comparison of cross-section profiles of cells shown in Figure 1.

Figure 3 shows the SEM images of the peripheral part of a cell on CNTs. Numerous filopodia 10–20 μm in length are extended and twisted on the CNT net with high density (Figure 3a). In the enlarged photograph (Figure 3b), the diameter of filopodia was comparable with CNTs and the apex of a filopodium is attached to the surface of CNTs.

In the present study, the difference of cell morphology on substrates with or without CNTs was investigated by SEM *in vitro*. Recently, toxicity of CNTs was reported;⁴ however, our previous studies showed the number of cells on CNTs was larger



Figure 3. High-magnification SEM images of the peripheral part of SaOS2 cell grown on CNTs. a: Numerous fine filopodia extend toward CNT scaffolds. b: The apex of a filopodium attached on CNTs (arrowhead).

than the number of disseminated cells after 3 days, and cells on CNTs were more proliferated than those on PC.⁵ The results of this study revealed that cells could adhere on CNTs and proliferate excellently.

The morphology of the cells with CNTs was markedly different from that of those without CNTs. Most of cells on CNTs were flat and spread in all directions. To evaluate the difference of cell morphology, quantitative analysis of cross-section profiles of cells was carried out using CLSM. The results showed that the length of cells on CNTs was as long as about 10 times that on PC, and the contact angle of cells on CNTs was less than one-sixth of that on PC. The cells on CNTs were clearly flatter. Additionally, the SEM images of cell periphery on CNTs revealed that numerous filopodia extended from cells toward the inside reticular CNTs. After treatment with trypsin to detach cells from CNTs, a few cells floated and showed a rounded-up shape. However, because of the mechanical binding of the filopodia extending from the cell bodies and twisted into CNT nets, most of the cells could not be detached from CNT scaffolds. The prominently flattered shape of cells, very small contact angle and growth of numerous filopodia suggested that CNTs had high affinity for adherence to human-derived osteoblastic cells. In contrast, few cells attached and grew on the graphite scaffolds. Although both CNTs and graphite consist of carbon, cell responses to them such as adhesion are quite different. Graphite is used as a material for heart valve prosthetics because it is nonthrombogenic. The difference of morphology between the fiber structure in CNTs and sheet structure in graphite would be one factor affecting their properties. The topology of the substrate affects the different aspects of cell behavior such as adhesion, proliferation, and morphology. Cell activity is influenced by microstructure and nanostructure. CNT scaffolds have a nanostructure, whereas PC membranes have a microstructure. The nanostructure, with its large surface area and high surface energy, may affect the

morphology of cells on CNTs. In addition to surface topography, surface chemistry also plays a role in cell adhesion, proliferation, and morphology.¹⁰ Various proteins such as extracellular matrix proteins and integrins may be related to cell adhesion. For example, the extracellular matrix of bone consists of collagenous proteins. In vitro, adsorption of proteins such as fibronectin and vitronectin in serum onto materials may influence cellular responses. The CNTs surface was reported to be coated with various adsorbed molecules.¹¹ One possible explanation might be that the difference cellular response to CNTs and PC were caused by the difference of adsorption of protein. The excellent cell attachment and growth with numerous filopodia suggest that CNTs could be potential materials for various biomedical uses.

This work was supported by Health and Labour Science Research Grants in Research on Advanced Medical Technology in Nanomedicine Area from the Ministry of Health, Labour and Welfare of Japan and by a Grant (No. 16390549) from the Ministry of Education, Culture, Sports, Science and Technology of Japan.

References

- 1 S. Iijima, *Nature* **1991**, *354*, 56.
- 2 A. Bianco, K. Kostarelos, C. D. Partidos, M. Prato, *Chem. Commun.* **2005**, 571.
- 3 Y. Sato, K. Shibata, H. Kataoka, S. Ogino, F. Bunshi, A. Yokoyama, K. Tamura, T. Akasaka, M. Uo, K. Motomiya, B. Jeyadevan, R. Hatakeyama, F. Watari, K. Tohji, *Mol. Biosyst.* **2005**, *1*, 142.
- 4 K. F. Soto, A. Carrasco, T. G. Powell, L. E. Murrin, K. M. Garza, *Mater. Sci. Eng.*, in press.
- 5 N. Aoki, A. Yokoyama, Y. Nodasaka, T. Akasaka, M. Uo, Y. Sato, K. Tohji, F. Watari, *J. Biomed. Nanotechnol.* **2005**, *1*, 402.
- 6 A. Yokoyama, Y. Sato, Y. Nodasaka, S. Yamamoto, T. Kawasaki, M. Shindoh, T. Kohgo, T. Akasaka, M. Uo, F. Watari, K. Tohji, *Nano Lett.* **2005**, *5*, 157.
- 7 M. Mattson, R. C. Haddon, A. M. Rao, *J. Mol. Neurosci.* **2000**, *14*, 175.
- 8 K. L. Elias, R. L. Price, T. J. Webster, *Biomaterials* **2002**, *23*, 3279.
- 9 Y. Sato, A. Yokoyama, K. Shibata, Y. Akimoto, S. Ogino, Y. Nodasaka, T. Kohgo, K. Tamura, T. Akasaka, M. Uo, K. Motomiya, B. Jeyadevan, M. Ishiguro, R. Hatakeyama, F. Watari, K. Tohji, *Mol. Biosyst.* **2005**, *1*, 176.
- 10 K. Anselme, *Biomaterials* **2000**, *21*, 667.
- 11 T. Akasaka, F. Watari, *Chem. Lett.* **2005**, *34*, 826.

A Novel DNA Vaccine Targeting Macrophage Migration Inhibitory Factor Protects Joints From Inflammation and Destruction in Murine Models of Arthritis

Shin Onodera,¹ Shigeki Ohshima,¹ Harukazu Tohyama,¹ Kazunori Yasuda,¹ Jun Nishihira,² Yoichiro Iwakura,³ Ikkei Matsuda,⁴ Akio Minami,¹ and Yoshikazu Koyama¹

Objective. Previous studies have demonstrated that neutralization of macrophage migration inhibitory factor (MIF) by anti-MIF antibodies decreases joint inflammation and destruction in a type II collagen-induced arthritis model in mice. The aim of this study was to develop and describe a simple and effective method of active immunization that induces anti-MIF autoantibodies, which may neutralize MIF bioactivity.

Methods. We developed a MIF DNA vaccine by introducing oligonucleotides encoding a tetanus toxoid (TTX) Th cell epitope into the complementary DNA sequence of murine MIF. Mice were injected with this construct in conjunction with electroporation. The ability of this immunization to inhibit the development of collagen antibody-induced arthritis (CAIA) in BALB/c mice and spontaneous autoimmune arthritis in interleukin-1 receptor antagonist (IL-1Ra)-deficient mice was then evaluated.

Results. Mice that received the MIF/TTX DNA vaccine developed high titers of autoantibodies that reacted to native MIF. Compared with unvaccinated mice, vaccinated mice also produced less serum tumor necrosis factor α after receiving an intravenous injection

of lipopolysaccharide. In addition, vaccination with MIF/TTX DNA resulted in significant amelioration of both CAIA in BALB/c mice and symptoms of autoimmune arthritis in IL-1Ra-knockout mice.

Conclusion. These results suggest that MIF/TTX DNA vaccination may be useful for ameliorating the symptoms of rheumatoid arthritis.

Recent reevaluation of macrophage migration inhibitory factor (MIF) has suggested that MIF may be an important mediator of various inflammatory diseases. In particular, increasing evidence suggests that MIF plays a key role in the pathogenesis of rheumatoid arthritis (RA) (1). For example, we previously reported that in the rheumatoid synovium, MIF is expressed exclusively in synovial T cells, and that MIF levels in joint fluid are much higher in patients with RA than in patients with osteoarthritis (OA) or normal volunteers (2). Moreover, MIF is known to induce macrophages to produce tumor necrosis factor α (TNF α) and nitric oxide (3) and has been shown to up-regulate matrix metalloproteinases and cyclooxygenase 2 messenger RNA in rheumatoid synovial fibroblasts (4,5). Furthermore, MIF-deficient mice are protected from antigen-induced arthritis and arthritis induced by anti-type II collagen antibodies (collagen antibody-induced arthritis [CAIA]) (6,7). In addition, both the synovial expression of MIF and polymorphisms in the MIF gene promoter have been reported to correlate positively with disease activity in RA (8,9). These observations strongly suggest that MIF plays an important role in the pathomechanism of RA.

Monoclonal antibodies to MIF have been shown to inhibit joint inflammation profoundly in rodent models of RA (10,11). However, the therapeutic utility of such monoclonal antibodies is limited by 1) the massive

Supported in part by grants-in-aid from the Ministry of Science and Education (no. 15591560), the Hip Joint Foundation of Japan, and the Uehara Memorial Foundation.

¹Shin Onodera, MD, Shigeki Ohshima, MD, Harukazu Tohyama, MD, Kazunori Yasuda, MD, Akio Minami, MD, Yoshikazu Koyama, PhD: Hokkaido University Graduate School of Medicine, Sapporo, Japan; ²Jun Nishihira, MD: GeneticLab Co., Sapporo, Japan; ³Yoichiro Iwakura, MD: Center for Experimental Medicine, Institute of Medical Science, University of Tokyo, Tokyo, Japan; ⁴Ikkei Matsuda: Institute for Genetic Medicine, Hokkaido University, Sapporo, Japan.

Address correspondence and reprint requests to Yoshikazu Koyama, PhD, Department of Biochemistry, Hokkaido University Graduate School of Medicine, Sapporo 060-8638, Japan. E-mail: y_koyama@med.hokudai.ac.jp.

Submitted for publication June 30, 2006; accepted in revised form November 9, 2006.

amounts of antibody that must be injected each time (which could generate transient undesirable local and systemic reactions); 2) the short duration of the protective effects because of a lack of immune B cell memory, which necessitates frequent injections; and 3) the fact that either humanized antibodies (which are usually of low affinity) or heterogeneous antibodies (the repeated administration of which will probably generate an anti-antibody response) would have to be used (12). To overcome these limitations, researchers have sought to develop therapeutic vaccines that will elicit autoantibodies against target proteins such as cytokines or pathogens.

The aim of the current study was to develop a vaccine that would generate endogenous anti-MIF antibodies. This was achieved by constructing the MIF/tetanus toxoid (TTX) DNA vaccine, which encodes a variant of murine MIF (mMIF), the second loop of which is replaced by a promiscuous Th cell epitope from tetanus toxin. The ability of this vaccine to inhibit the development of arthritis was tested in 2 different murine arthritis models. One of these models is CAIA, which is induced in BALB/c mice by injection with a cocktail of anti-type II collagen monoclonal antibodies followed by an injection of lipopolysaccharide (LPS). This is a self-limiting arthritis, the symptoms of which last for ~3–4 weeks after administration of the monoclonal antibodies. The other model involves interleukin-1 receptor antagonist (IL-1Ra)-deficient mice, which at ~5 weeks of age spontaneously develop an autoimmune polyarthritis that is characterized by enhanced levels of serum autoantibodies against immunoglobulin, type II collagen, and double-stranded DNA. In close to 100% of the mice in both models, arthritis develops in the limb joints.

MATERIALS AND METHODS

Mice. BALB/c mice (4 weeks old) were purchased from Sankyo Laboratory Service (Shizuoka, Japan) and were maintained under specific pathogen-free conditions. IL-1Ra-knockout mice were generated as previously described (13). All animal procedures were conducted according to the guidelines of the Hokkaido University Institutional Animal Care and Use Committee under an approved protocol. Female adult mice (4 weeks of age) were used in each experiment.

Construction of the MIF/TTX expression plasmid. Murine MIF complementary DNA (cDNA) was cloned into the mammalian expression vector pCAGGS (14). To generate an immunologically active MIF antigen, an MIF variant whose second loop region is replaced by a TTX Th cell epitope was designed. For this purpose, the cDNA region that encodes the second loop of mMIF (amino acids 32–37 [GKPAQY]) was deleted from the MIF cDNA and substituted with an *Eco* RI

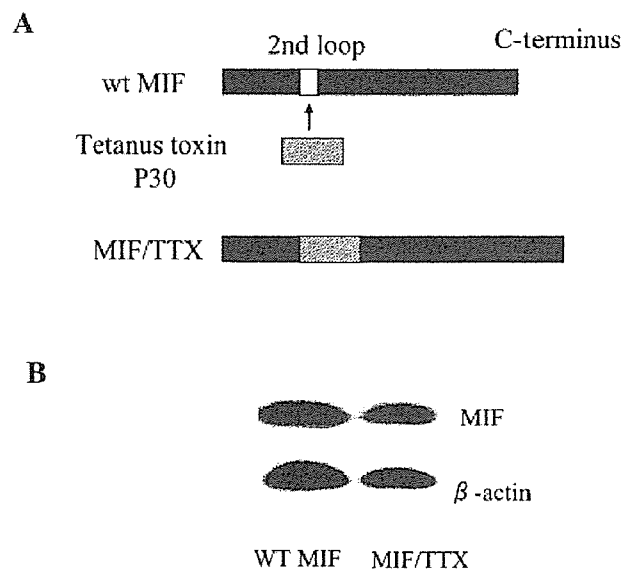


Figure 1. Design and antigenicity of the macrophage migration inhibitory factor (MIF)/tetanus toxoid (TTX) DNA vaccine. **A**, Design of a DNA construct that expresses a murine MIF (mMIF) variant, the second loop of which bears a promiscuous Th cell epitope from TTX. To generate this construct, mMIF cDNA was cloned into the mammalian expression vector pCAGGS, after which the second loop region of MIF cDNA was substituted with the Th cell epitope. **B**, Expression and antigenicity of wild-type (WT) MIF and MIF/TTX DNAs. COS-7 cells were transiently transfected with the DNA constructs expressing either WT MIF or MIF/TTX, and their lysates were analyzed by Western blotting using rabbit anti-mMIF antibody. Results are representative of 3 independent experiments.

site by standard polymerase chain reaction-based techniques. Complementary DNA encoding the TTX p30 Th cell epitope (FNNFTVSFWRVLPKVSASHL) (15) with an *Eco* RI site at both termini was obtained by hybridization of partially overlapping oligo DNAs (sense, GAATTCAACAACCTTCACCGTGAGCTTCTGGCTGCGCGTGCCCAA; anti-sense, GGAATCCAGGTGGCTGCGGCTCACCTTGGGCACGCGCAGCCAGA) and subsequent polymerization with the *Klenow* fragment of DNA polymerase. After digestion with *Eco* RI, the p30 cDNA was inserted into the *Eco* RI site of the MIF expression plasmid (Figure 1), and a clone bearing a correctly oriented insert was selected. The MIF/TTX plasmid DNA was then purified by alkaline lysis followed by 2 rounds of CsCl density-gradient ultracentrifugation. This preparation was used for animal vaccination.

Analysis of in vitro expression of MIF/TTX. COS-7 cells were transfected with either the expression plasmid for wild-type (WT) MIF or MIF/TTX by using Effectene transfection reagent (Qiagen, Valencia, CA) according to the method recommended by the manufacturer. After 24 hours, the cells were lysed with 1% Nonidet P40/20 mM Tris HCl, pH 7.6/20% glycerol/1 mM EDTA/1 mM phenylmethylsulfonyl fluoride. The extracts were then subjected to sodium dodecyl sulfate-polyacrylamide gel electrophoresis and blotted onto

polyvinylidene difluoride membranes, which were subsequently blocked with 3% skim milk and then incubated with rabbit anti-MIF antibody. After reacting the membranes with horseradish peroxidase (HRP)-conjugated donkey anti-rabbit antibody, the MIF protein was visualized by using a chemiluminescence system (Amersham, Arlington Heights, IL).

Intramuscular DNA injection and electroporation.

Gene transfer into muscle by electroporation was performed essentially as described previously (16). Mice were anesthetized with ether and shaved around their hind legs, after which a pair of electrode needles (5-mm gap and 0.5-mm diameter; Nepa Gene, Chiba, Japan) were inserted into an anterior tibial muscle, and the DNA vaccine (25 μ g/25 μ l 0.9% saline) was injected into the portion between the needles. Three electric pulses (50V and 50 msec) were applied by using an electric pulse generation system (T820 and Optimizer 500; BTX, San Diego, CA) and were followed by another 3 pulses with inverted polarity. The other tibial muscle was then also injected and subjected to electroporation. As a result, each mouse received 50 μ g of the naked plasmid. A similar vaccination procedure was repeated 3 weeks later.

Evaluation of anti-MIF antibody titers in sera from DNA-vaccinated mice. Anti-MIF titers in plasma were determined by direct enzyme-linked immunosorbent assay (ELISA). Briefly, individual plasma samples from vaccinated mice were collected from the tail vein and diluted with 0.1% bovine serum albumin/phosphate buffered saline (PBS)/0.05% Tween 20. Small aliquots of diluted plasma (1:200) were added to 96-well flat-bottomed plates precoated with recombinant mMIF. The serum anti-MIF antibodies that reacted with the precoated MIF were detected by HRP-conjugated goat anti-mouse antibody, followed by color development with a substrate reagent (Techne, Minneapolis, MN). Antibodies raised in the vaccinated animals were also tested for their ability to compete with a specific mouse monoclonal antibody for MIF antigen. Thus, microtiter plates were precoated with the anti-MIF monoclonal antibody XIV.14.3 (a kind gift from Dr. Richard Bucala, Yale University). The pooled plasma samples from animals that had been vaccinated with the MIF/TTX vaccine or the control pCAGGS plasmid were serially diluted and preincubated with recombinant mMIF. The reaction mixtures were then added to the microtiter plate, incubated for 1 hour, and washed. The amount of MIF bound by the XIV.14.3 monoclonal antibody was then determined by serial incubation, first with biotin-labeled rabbit anti-MIF antibody and then with HRP-conjugated biotin-streptavidin complex (Amersham).

Measurement of serum TNF α . It has been reported that, compared with untreated mice, mice treated with a polyclonal anti-MIF antibody produce less serum TNF α after intravenous injection with LPS (17). We tested whether the anti-MIF antibodies raised by MIF/TTX DNA vaccination have the same suppressive activity. Thus, 6 weeks after administering the MIF/TTX vaccine or the control pCAGGS construct once to 4-week-old BALB/c mice, each mouse was injected intravenously with 200 μ l of a mixture of LPS (0111:B4; 1 μ g/ml) and D-galactosamine (60 mg/ml). Blood samples (5 μ l) were then collected from the tail vein every 1.5 hours, and serum concentrations of TNF α were measured by using a mouse TNF α ELISA kit (BioSource, Camarillo, CA) according to the manufacturer's protocol.

Initiation of CIA and evaluation of arthritis. Arthritis antibody kits were obtained from Immuno-Biological Laboratories (Gumma, Japan), and arthritis was induced according to the manufacturer's instructions (18). Briefly, 2 weeks after receiving their second DNA immunization, BALB/c mice were injected intraperitoneally with a mixture of 4 anti-type II collagen monoclonal antibodies (2 mg each), followed by intraperitoneal injection with 50 μ g of LPS (0111:B4) 3 days later (day 0). The incidence of arthritis was judged macroscopically by examining each joint for swelling and redness on days 1, 3, 7, 14, and 21, as described previously (19), and each joint was graded as follows: grade 0 = normal, grade 1 = light swelling of the joint and/or redness of the footpad, grade 2 = obvious swelling of the joint, and grade 3 = severe swelling and fixation of the joint. The arthritis score was calculated for all 4 limbs; thus, the maximum possible score for each mouse was 12 points.

Evaluation of arthritis in IL-1Ra-knockout mice. IL-1Ra-knockout mice were vaccinated once with MIF/TTX (n = 16) at the age of 4 weeks. Control mice were injected once with the pCAGGS vector (n = 5) or endotoxin-free saline (n = 6). The anti-mMIF titers in sera were assessed every 2 weeks, as previously described. The clinical parameters assessed were the percentage of arthritic mice, the arthritis score, and paw swelling. The arthritis score was evaluated as described above. Paw swelling was assessed by measuring the thickness of the affected hind paws with 0–10-mm calipers (Mitutoyo, Kana-gawa, Japan).

Histopathology. BALB/c mice given anti-type II collagen monoclonal antibodies were killed under anesthesia on day 14, while IL-1Ra-knockout mice were killed 16 weeks after being given the DNA vaccine. The whole hind limbs of the mice were harvested, fixed in 4% paraformaldehyde in PBS, decalcified in EDTA, and then embedded in paraffin. Serial sagittal sections were subjected to hematoxylin and eosin staining for histologic analyses. For IL-1Ra-knockout mice, Safranin O and fast green/iron hematoxylin staining was added to estimate the loss of cartilage proteoglycan. Moreover, MIF protein expression was examined by immunohistochemistry using an anti-MIF antibody, as described previously (6).

Statistical analysis. For statistical analysis, one-way factorial analysis of variance was performed, followed by Fisher's protected least significant difference as a post hoc test.

RESULTS

Design of the MIF/TTX vaccine and analysis of its *in vitro* expression. We constructed a DNA vaccine that encoded an mMIF variant whose second loop region was replaced with a promiscuous foreign Th cell epitope from TTX (FNNFTVSFWLRVVPKVSASHL) (Figure 1A). The second loop region of MIF (aa ³²Gly–³⁷Tyr) was selected for TTX epitope insertion on the basis of the 3-dimensional structure of MIF (20); replacement of this region rather than the other loops seemed less likely to interfere with the quaternary structure and antigenicity of the trimeric MIF complex. The chimeric MIF/TTX cDNA construct was then

cloned into the expression plasmid pCAGGS. Prior to in vivo administration, we tested whether this construct produced the right protein by transiently transfecting COS-7 cells. As shown in Figure 1B, the chimeric MIF/TTX protein showed mobility on a sodium dodecyl sulfate electrophoresis gel similar to that of WT MIF. Moreover, it was recognized by a rabbit antibody raised against WT mMIF. Thus, insertion of the foreign Th cell epitope did not affect expression of the molecule or the antigenicity of its MIF domain.

Generation of anti-MIF antibodies and production of serum TNF α in MIF/TTX-vaccinated BALB/c mice upon injection with LPS. We tested whether the DNA vaccine could induce a polyclonal antibody response that recognized native MIF. Thus, both tibial muscles of BALB/c mice were vaccinated intramuscularly with 50 μ g of WT MIF, MIF/TTX, or vector DNA in 0.9% saline, with the aid of electroporation. The animals were vaccinated twice, 3 weeks apart. As shown in Figure 2A, by 4 weeks after the first vaccination, the MIF/TTX-vaccinated mice had autoantibodies that reacted to native MIF. In contrast, neither the WT MIF vaccine nor the vector vaccine raised such MIF-reactive antibodies until 12 weeks after the first vaccination. These differences were statistically significant ($P < 0.05$, MIF/TTX versus pCAGGS) and indicate that by incorporating the TTX Th cell epitope, the immunologic tolerance of mice to the MIF self protein is bypassed.

We also tested whether the anti-MIF antibodies generated by the MIF/TTX DNA vaccine could compete with a MIF-specific monoclonal antibody for the binding of native mMIF protein. A competition ELISA revealed that when the polyclonal serum antibodies from vaccinated mice were preincubated with recombinant mMIF, they could compete with anti-MIF monoclonal antibody 14.3 for binding to the MIF protein (Figure 2B).

It has been shown previously that pretreatment of mice with a polyclonal anti-MIF antibody effectively suppresses the rise in serum TNF α levels that is induced by a subsequent intravenous injection of LPS (17). Thus, we tested whether the MIF/TTX vaccine-induced anti-MIF antibodies would also have the same effect. We observed that when mice vaccinated once with MIF/TTX were injected with LPS 6 weeks after the vaccination, their serum TNF α levels were significantly lower than those of LPS-treated mice injected previously with vector DNA (Figure 2C) ($P < 0.0001$, MIF/TTX versus pCAGGS). Thus, the anti-MIF antibodies generated by the MIF/TTX DNA vaccine have antiinflammatory properties, probably because they inhibit the bioactivity of endogenous MIF.

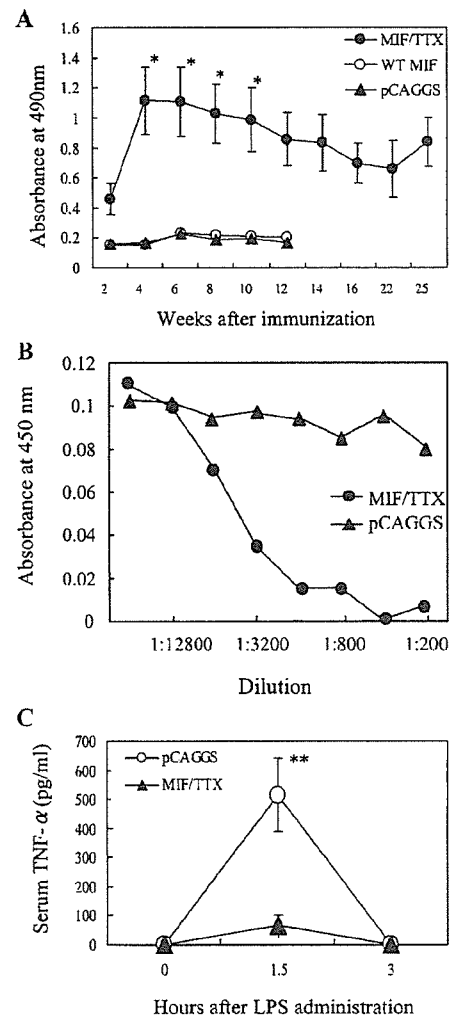


Figure 2. A, Effects of immunization with MIF/TTX DNA on elicitation of autoantibodies that recognize native mMIF. BALB/c mice were vaccinated twice, 3 weeks apart, with 50 μ g of pCAGGS, WT MIF construct, or MIF/TTX construct in 0.9% endotoxin-free sterile saline ($n = 5$ mice per group). Serum samples from these mice were obtained at various time points, and anti-MIF antibody levels were measured by enzyme-linked immunosorbent assay (ELISA), using microtiter plates coated with recombinant mMIF. * = $P < 0.05$, MIF/TTX versus pCAGGS. B, Ability of polyclonal anti-MIF antibodies generated by MIF/TTX DNA vaccination to compete with anti-MIF monoclonal antibody 14.3 for binding to recombinant MIF. A competitive ELISA was performed by preincubating pooled sera from the pCAGGS- or MIF/TTX-vaccinated mice described in A with recombinant mMIF and then adding the mixtures to a microtiter plate on which monoclonal antibody 14.3 had been immobilized. C, Effect of MIF/TTX DNA vaccination on lipopolysaccharide (LPS)-induced rise in serum tumor necrosis factor α (TNF α) levels. Mice immunized with MIF/TTX or vector DNA were injected intravenously with LPS 6 weeks after the vaccination. Serum TNF α levels were measured by ELISA. Values are the mean \pm SEM. ** = $P < 0.0001$, MIF/TTX versus pCAGGS. See Figure 1 for other definitions.

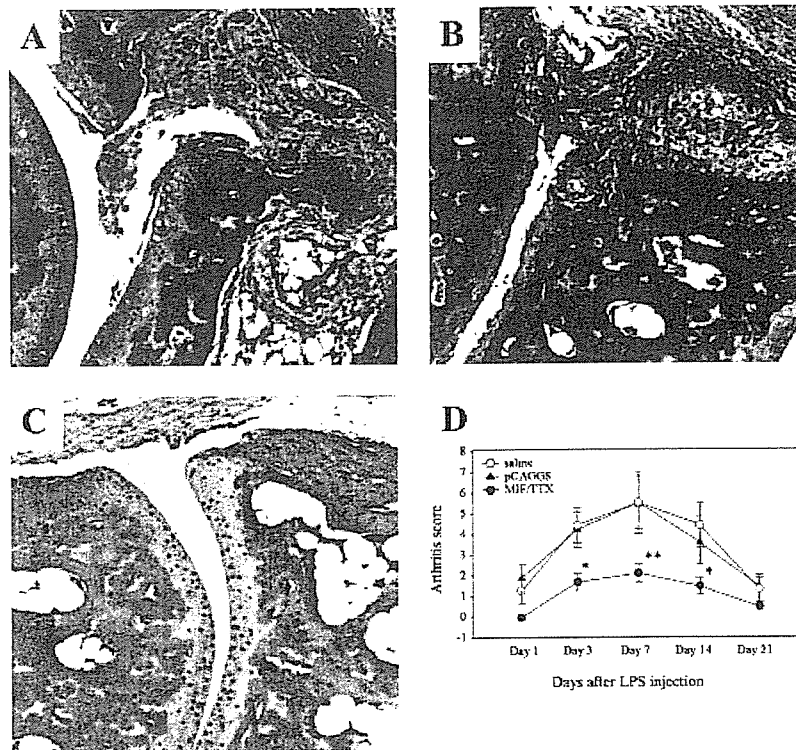


Figure 3. Representative results of histologic analysis of tarsocrural joints from **A**, saline-treated, **B**, pCAGGS-vaccinated, and **C**, MIF/TTX-vaccinated BALB/c mice on day 14. Marked changes were observed in specimens obtained from saline-treated and pCAGGS-vaccinated mice, including synovial hyperplasia, inflammatory cell infiltration, extensive pannus formation at the cartilage–bone junction, and severe cartilage destruction. Specimens obtained from some of the MIF/TTX-vaccinated mice revealed only slight thickening and proliferation of the synovial lining, mild inflammatory cell infiltration, no pannus invasion, and intact bone and cartilage structure. (Original magnification $\times 200$.) **D**, Arthritis scores (degree of arthritis in all 4 joints of each mouse) following injection of lipopolysaccharide (LPS). Values are the mean \pm SEM. * = $P < 0.05$, ** = $P < 0.005$, MIF/TTX versus pCAGGS. See Figure 1 for other definitions.

We also attempted to measure the ability of the immune sera to inhibit the *in vitro* production of TNF α by LPS-stimulated peritoneal macrophages. However, reproducible results could not be obtained, possibly because the sera interfered nonspecifically with TNF α production. A similar failure has been reported previously (21). Nevertheless, these observations together indicate that immunization with MIF/TTX DNA generated antibodies that can specifically recognize native mMIF and probably neutralize the bioactivity of this molecule.

Effect of vaccination with MIF/TTX DNA on the development and severity of CIA. In mice with CIA, the endogenous production of MIF is enhanced, and antibodies to MIF have been shown to profoundly inhibit joint inflammation (7). Thus, we tested whether

the MIF/TTX DNA vaccine would inhibit the development of CIA in this murine model of rheumatoid arthritis by immunizing 16 BALB/c mice twice with MIF/TTX DNA. As controls, we also immunized 6 mice with saline and 5 mice with pCAGGS vector. For histologic evaluation, 3 groups consisting of 3–4 BALB/c mice, respectively, were prepared as described above. Two weeks after the second immunization, the mice were injected first with anti-type II collagen monoclonal antibodies and then 3 days later were injected with LPS.

Histologic analysis of the saline- or pCAGGS-treated mice on day 14 revealed marked pathologic changes in the tarsocrural joint tissues; these changes included synovial hyperplasia, inflammatory cell infiltra-

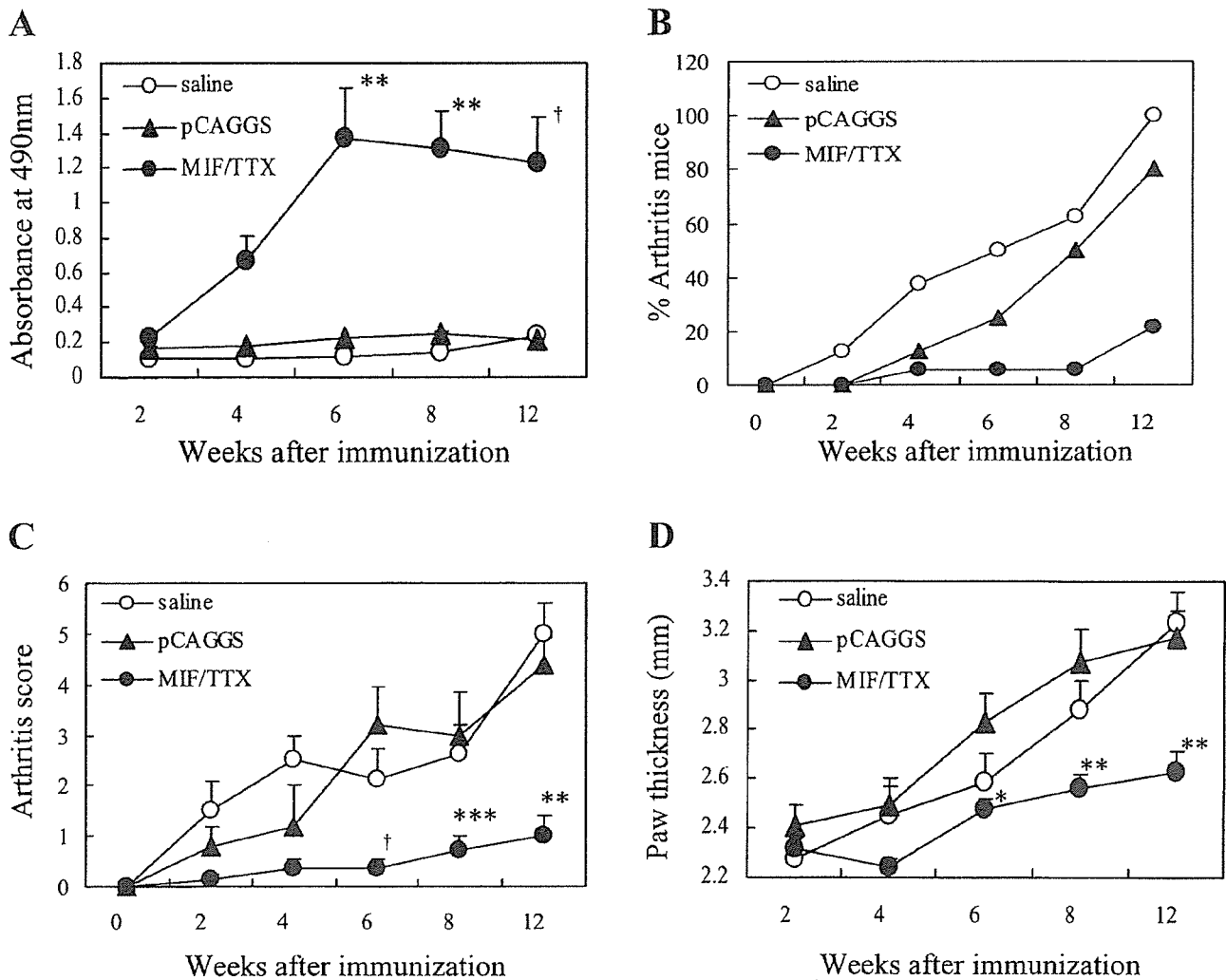


Figure 4. The MIF/TTX DNA vaccine inhibits the development of spontaneous autoimmune arthritis in interleukin-1 receptor antagonist (IL-1Ra)-knockout mice and reduces its severity. Four-week-old IL-1Ra-knockout mice were vaccinated once with MIF/TTX ($n = 16$), pCAGGS vector ($n = 5$), or endotoxin-free saline ($n = 6$). A, Anti-mMIF serum titers. B, Percentage of arthritic mice. C, Arthritis score. D, Degree of hind paw swelling. Values are the mean and SEM. * = $P < 0.05$; ** = $P < 0.0001$; *** = $P < 0.001$; † = $P < 0.005$, MIF/TTX versus pCAGGS. See Figure 1 for other definitions.

tion, extensive pannus formation at the cartilage-bone junction, and severe cartilage destruction (Figures 3A and B). In contrast, histologic sections of the tarsocrural joints from some of the MIF/TTX-vaccinated mice revealed only slight thickening and proliferation of the synovial lining, mild inflammatory cell infiltration, no pannus invasion, and intact bone and cartilage structure (Figure 3C). Moreover, among animals examined on days 3, 7, and 14, the MIF/TTX-vaccinated mice had significantly lower arthritis scores compared with controls, which indicated that the severity of clinical symp-

toms of arthritis was reduced in these animals ($P < 0.05$ and $P < 0.005$, MIF/TTX versus pCAGGS) (Figure 3D).

Effect of vaccination with MIF/TTX DNA on the development of autoimmune arthritis in IL-1Ra-knockout mice. We also examined whether the MIF/TTX vaccine can act to block the severity of spontaneous arthritis in IL-1Ra-knockout mice. Thus, we immunized IL-1Ra-knockout mice with MIF/TTX DNA, pCAGGS DNA, or saline once at age 4 weeks. Analysis of the anti-MIF antibody titers generated over time in these mice revealed significantly elevated titers 6

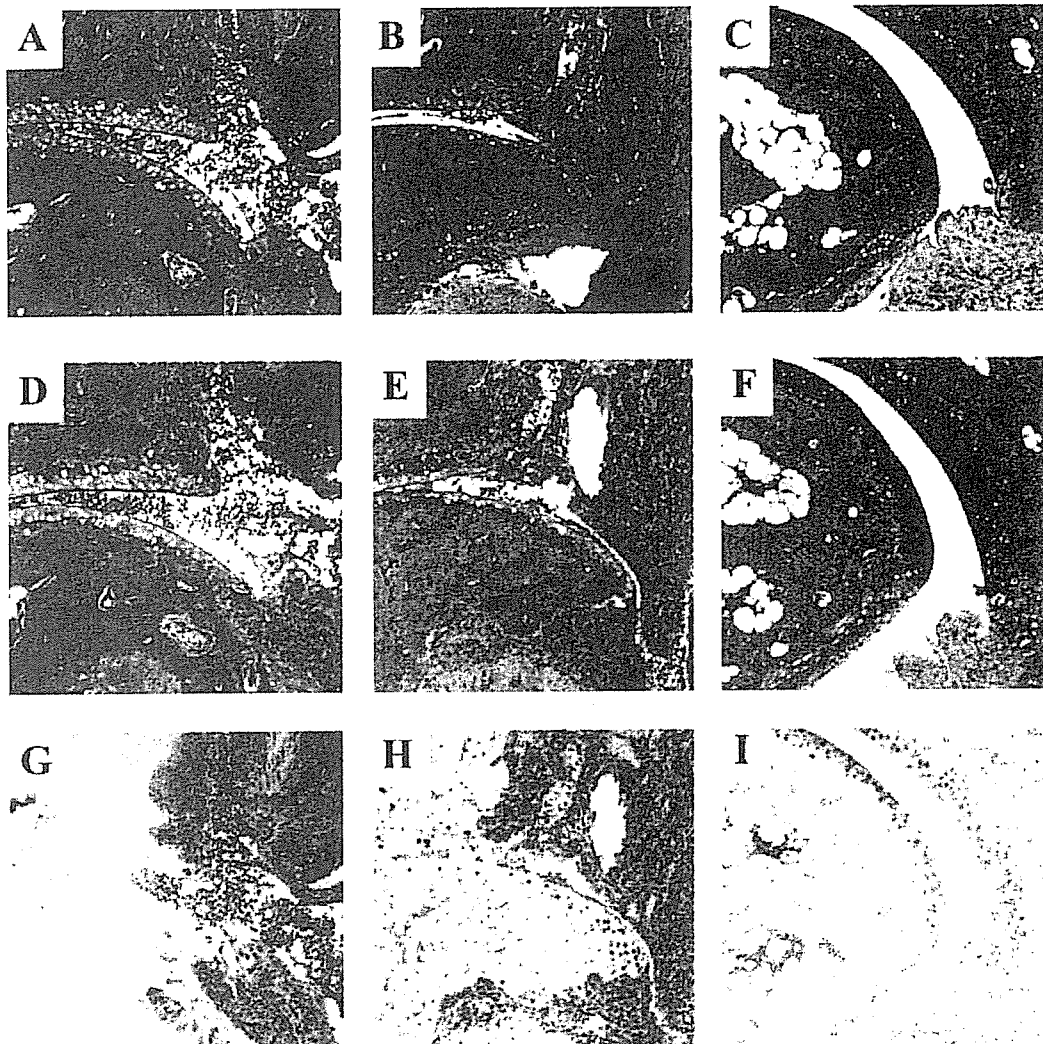


Figure 5. Representative results of histologic analysis of the effects of vaccination with saline (A, D, and G), pCAGGS (B, E, and H), or macrophage migration inhibitory factor/tetanus toxoid (C, F, and I). Ankle joints from interleukin-1 receptor antagonist (IL-1Ra)-knockout mice were collected 16 weeks after vaccination, and specimens were stained with hematoxylin and eosin (A–C) or Safranin O (D–F), or were immunohistologically stained with polyclonal anti-MIF antibodies (G–I). (Original magnification $\times 200$.)

weeks after the vaccination; these elevated levels were maintained for at least another 6 weeks (Figure 4A). The clinical severity of autoimmune arthritis in the animals was determined by estimating the arthritis score and the degree of hind paw swelling. The percentage of arthritic mice at the indicated time points was also determined.

Twelve weeks after immunization, the percentage of arthritic mice among animals vaccinated with MIF/TTX was reduced to 20%, compared with 100% of mice receiving saline and 80% of mice immunized with

pCAGGS (Figure 4B). Mice vaccinated with MIF/TTX also had significantly lower arthritis scores at 6, 8, and 12 weeks after the vaccination (Figure 4C). The mean paw thickness of the MIF/TTX-vaccinated animals was also significantly lower at 6, 8, and 12 weeks after vaccination compared with that of the pCAGGS-vaccinated mice (Figure 4D). At week 16 after vaccination, histologic examination of the affected ankle joints from saline-treated IL-1Ra-knockout mice revealed severe synovitis, pannus formation, cartilage/bone erosion, and positive immunostaining for MIF in the synovium and

pannus (Figures 5A, D, and G). The affected ankle joints from pCAGGS-vaccinated mice also showed severe synovitis, pannus formation, cartilage/bone erosion, and positive immunostaining for MIF within the synovium and pannus (Figures 5B, E, and H). In contrast, the affected ankle joints from MIF/TTX-vaccinated mice showed only very mild synovitis, cartilage/bone erosion, loss of Safranin O staining of the cartilage, and immunostaining for MIF (Figures 5C, F, and I).

DISCUSSION

In this study, we have shown that active vaccination against MIF could be a novel approach for the treatment of RA and, potentially, other autoimmune disorders as well. It is well known that RA is associated with the abnormally persistent production of TNF α and other proinflammatory cytokines, including interleukin-6 (IL-6), IL-8, and IL-1 (22), in inflamed joint tissue. We focused on MIF as a therapeutic target for RA for the following reasons. First, MIF up-regulates TNF α production by macrophages (2). Second, MIF-deficient mice generate lower amounts of inflammatory cytokines such as TNF α in response to LPS stimulation (23). Third, medium conditioned by cultured rheumatoid synovial fibroblasts induces peripheral blood mononuclear cells to release TNF α ; this effect is blocked by anti-MIF antibodies (24). These observations indicate that MIF may be a key upstream regulator of synovial inflammation in RA (24). Thus, suppressing MIF activity may be a more effective manner of treating RA than is suppression of other inflammatory cytokines.

The pathogenesis of the CAIA model may differ somewhat from that of RA in that type II collagen-specific T cells are unlikely to be involved in CAIA; moreover, the initiation of CAIA also requires injection with LPS. However, this experimental model of arthritis has many advantages, namely, this model can cause arthritis with 100% probability in many strains of mice irrespective of their major histocompatibility complex type and within a short period of time (18). Moreover, it has been reported that MIF plays an important role in the pathogenesis of the CAIA model (7,25). However, this model may not be the best one for evaluating the therapeutic effect of MIF DNA vaccination over a long period, because CAIA lasts, at most, 3–4 weeks, which is too short a time period for such an evaluation.

IL-1Ra is an endogenous inhibitor of IL-1, and polyarthritis spontaneously develops in IL-1Ra-knockout mice on the BALB/c background, starting at 5

weeks of age. By 12 weeks of age, almost all mice have affected joints (19). The histopathologic features of the lesions closely resembles those in human RA, because marked synovial and periarticular inflammation and articular erosion caused by invasion of granulation tissues are observed. In this model, excess IL-1 signaling due to the lack of IL-1Ra induces T cell-mediated autoimmunity that results in joint-specific inflammation and bone destruction. Therefore, this model, which is characterized by long disease duration, may be suitable for evaluating over a long period of time the prophylactic effect of a particular approach. Consequently, we investigated the effect of MIF/TTX DNA vaccination on the arthritis in this murine model. Our experiments revealed that a single vaccination with MIF/TTX DNA was sufficient to suppress the incidence and severity of arthritis for at least 12 weeks.

How neutralization of MIF suppresses the development of arthritis in IL-1Ra-knockout mice, which is caused by excess IL-1 signaling, remains to be elucidated. Horai et al (19,26) reported that the joints of IL-1Ra-knockout animals have high levels of proinflammatory cytokines such as IL-1 β , IL-6, and TNF α , and that inhibiting TNF α function effectively suppresses the development of arthritis in these animals. This suggests that a proinflammatory cytokine network promotes the development of this autoimmune arthritis. Thus, it is possible that MIF, which is known to up-regulate the production of TNF α (3,23,24), may be a prominent upstream component of this network. This hypothesis will need to be tested in additional studies.

The Th cell-modified vaccine approach we used in the current study demonstrates the therapeutic potential of vaccines that generate immune responses against pathogenic self proteins. By incorporating a promiscuous foreign Th cell epitope into self proteins, the immunologic tolerance to self proteins can be bypassed (27–29). DNA vaccines represent a novel means of expressing antigens *in vivo* that will generate both humoral and cell-mediated immune responses, and the efficacy of DNA vaccines in preclinical animal models has been well documented (30). DNA vaccines have an advantage over recombinant protein vaccines in that the construction and purification of vectors for DNA vaccination are relatively simple. This approach is thus likely to increase the speed and decrease the effort required to develop novel protein vaccines. Moreover, this approach is useful for rapidly screening potential protein immunogens.

Naked cDNA encoding CC chemokines without

a Th cell epitope has been shown to elicit autoantibodies that effectively prevent the development of experimental adjuvant-induced encephalitis (31). The finding that autoantibodies could be generated without the help of a Th cell epitope may be related to the fact that oligonucleotide sequences in the plasmid, such as unmethylated CpG motifs, have been shown to be able to act as immune adjuvant, thereby accelerating antigen-specific immune responses (32). However, Hertz et al (33) reported that unmodified wild-type murine IL-5 cDNA failed to elicit antibodies, which is consistent with the inability of wild-type mMIF cDNA to elicit autoantibodies in the current study.

Thus, the proper selection of a Th cell epitope and its insertion into the appropriate sites of the cDNA may be the key to the successful design of an effective DNA vaccine. Moreover, DNA delivery and DNA vaccine potency may be enhanced by electroporation. Supporting this possibility is the study by Selby et al (34), who reported that mice injected intramuscularly with a plasmid showed a 7.3-fold increase in luciferase expression and 8- to 20-fold enhanced antibody titers when they had also been subjected to electroporation at the time of immunization.

Active immunization with the MIF/TTX DNA vaccine reduced the symptoms of CAIA to the same extent as did therapeutically injected anti-mMIF monoclonal antibodies (7). Our preliminary safety studies, in which we monitored organ weights and the general histologic features of selected tissue, including the liver, kidney, and skin, did not reveal differences between unvaccinated and MIF/TTX DNA-vaccinated mice (data not shown). Similarly, significant differences in the wound-healing ability of mice in the 2 groups were not detected (data not shown). Additional safety studies, including hematologic examinations, are under way.

In conclusion, administration of Th cell-modified MIF DNA is a cost-effective, potentially prophylactic method of vaccination that can inhibit CAIA and spontaneous arthritis in IL-1Ra-knockout mice. Thus, active vaccination against MIF is a novel approach to the treatment of RA and possibly other autoimmune diseases as well.

AUTHOR CONTRIBUTIONS

Dr. Koyama had full access to all of the data in the study and takes responsibility for the integrity of the data and the accuracy of the data analysis.

Study design. Drs. Onodera, Nishihira, and Koyama.

Acquisition of data. Drs. Onodera, Oshima, and Iwakura, Mr. Matsuda, and Dr. Koyama.

Analysis and interpretation of data. Drs. Onodera and Koyama.

Manuscript preparation. Drs. Onodera, Yasuda, Minami, and Koyama.

Statistical analysis. Drs. Onodera and Tohyama.

REFERENCES

- Morand EF. New therapeutic target in inflammatory disease: macrophage migration inhibitory factor. *Intern Med J* 2005;35:419–26.
- Onodera S, Tanji H, Suzuki K, Kaneda K, Mizue Y, Sagawa A, et al. High expression of macrophage migration inhibitory factor in the synovial tissues of rheumatoid joints. *Cytokine* 1999;11:163–7.
- Bernhagen J, Mitchell RA, Calandra T, Voelker W, Cerami A, Bucala R. Purification, bioactivity, and secondary structure analysis of mouse and human macrophage migration inhibitory factor (MIF). *Biochemistry* 1994;33:14144–55.
- Onodera S, Kaneda K, Mizue Y, Koyama Y, Fujinaga M, Nishihira J. Macrophage migration inhibitory factor (MIF) up-regulates expression of matrix metalloproteinases in synovial fibroblasts of rheumatoid arthritis. *J Biol Chem* 2000;275:444–50.
- Sampey AV, Hall PH, Mitchell RA, Metz CN, Morand EF. Regulation of synoviocyte phospholipase A₂ and cyclooxygenase 2 by macrophage migration inhibitory factor. *Arthritis Rheum* 2001;44:1273–80.
- Leech M, Lacey D, Xue JR, Santos L, Hutchinson P, Wolvetang E, et al. Regulation of p53 by macrophage migration inhibitory factor in inflammatory arthritis. *Arthritis Rheum* 2003;48:1881–9.
- Ichiyama H, Onodera S, Nishihira J, Ishibashi T, Nakayama T, Minami A, et al. Inhibition of joint inflammation and destruction induced by anti-type II collagen antibody/lipopolysaccharide (LPS)-induced arthritis in mice due to deletion of macrophage migration inhibitory factor (MIF). *Cytokine* 2004;26:187–94.
- Morand EF, Leech M, Wedon H, Metz C, Bucala R, Smith MD. Macrophage migration inhibitory factor in rheumatoid arthritis: clinical correlations. *Rheumatology* 2002;41:558–62.
- Baugh JA, Chitnis S, Donnelly SC, Monteiro J, Lin X, Plant BJ, et al. A functional promoter polymorphism in the macrophage migration inhibitory factor (MIF) gene associated with disease severity in rheumatoid arthritis. *Genes Immun* 2002;3:170–6.
- Mikulowska A, Metz CN, Bucala R, Holmdahl R. Macrophage migration inhibitory factor is involved in the pathomechanism of collagen type-II induced arthritis in mice. *J Immunol* 1997;158:5514–7.
- Leech M, Metz CN, Santos L, Peng T, Holdsworth SR, Bucala R, et al. Involvement of macrophage migration inhibitory factor in the evolution of rat adjuvant arthritis. *Arthritis Rheum* 1998;41:910–7.
- Clark M. Antibody humanization: a case of the 'Emperor's new clothes'? *Immunol Today* 2000;21:397–402.
- Horai R, Asano M, Sudo K, Kanuka H, Suzuki M, Nishihara M, et al. Production of mice deficient in genes for interleukin (IL)-1 α , IL-1 β , IL-1 α/β , and IL-1 receptor antagonist shows that IL-1 β is crucial in turpentine-induced fever development and glucocorticoid secretion. *J Exp Med* 1998;187:1463–75.
- Niwa H, Yamamura K, Miyazaki J. Efficient selection for high-expression transfectants with a novel eukaryotic vector. *Gene* 1991;108:193–200.
- Panina-Bordignon P, Tan A, Termijtelen A, Demotz S, Corradin G, Lanzavecchia A. Universally immunogenic T cell epitopes: promiscuous binding to human MHC class II and promiscuous recognition by T cells. *Eur J Immunol* 1989;19:2237–42.

16. Aihara H, Miyazaki J. Gene transfer into muscle by electroporation in vivo. *Nature Biotech* 1998;16:867-70.
17. Kobayashi S, Nishihira J, Watanabe S, Todo S. Prevention of lethal acute hepatic failure by antimacrophage migration inhibitory factor antibody in mice treated with bacille Calmette-Guerin and lipopolysaccharide. *Hepatology* 1999;29:1752-9.
18. Terato K, Harper DS, Griffiths MM, Hasty DL, Ye XJ, Cremer MA, et al. Collagen-induced arthritis in mice: synergistic effect of *E. coli* lipopolysaccharide bypasses epitope specificity in the induction of arthritis with monoclonal antibodies to type II collagen. *Autoimmunity* 1995; 22:137-47.
19. Horai R, Saijo S, Tanioka H, Nakae S, Sudo K, Okahara A, et al. Development of chronic inflammatory arthropathy resembling rheumatoid arthritis in interleukin 1 receptor antagonist-deficient mice. *J Exp Med* 2000;191:313-20.
20. Suzuki M, Sugimoto H, Nakagawa A, Tanaka I, Nishihira J, Sakai M. Crystal structure of the macrophage migration inhibitory factor from rat liver. *Nature Struct Biol* 1996;3:259-66.
21. Spohn G, Schwarz K, Maurer P, Illges H, Rajasekaran N, Choi Y, et al. Protection against osteoporosis by active immunization with TRANCE/RANKL displayed on virus-like particles. *J Immunol* 2005;175:6211-8.
22. Brennan FM, Chantry D, Jackson A, Maini R, Feldmann M. Inhibitory effect of TNF α antibodies on synovial cell interleukin-1 production in rheumatoid arthritis. *Lancet* 1989;2:244-7.
23. Bozza M, Satoskar AR, Lin G, Lu B, Humbles AA, Gerard C, et al. Targeted disruption of migration inhibitory factor gene reveals its critical role. *J Exp Med* 1999;189:341-6.
24. Leech M, Metz C, Hall P, Hutchinson P, Gianis K, Smith M, et al. Macrophage migration inhibitory factor in rheumatoid arthritis: evidence of proinflammatory function and regulation by glucocorticoids. *Arthritis Rheum* 1999;42:1601-8.
25. Onodera S, Nishihira J, Koyama Y, Majima T, Aoki Y, Ichiyama H, et al. Macrophage migration inhibitory factor up-regulates the expression of interleukin-8 messenger RNA in synovial fibroblasts of rheumatoid arthritis patients: common transcriptional regulatory mechanism between interleukin-8 and interleukin-1 β . *Arthritis Rheum* 2004;50:1437-47.
26. Horai R, Nakajima A, Habiro K, Kotani M, Nakae S, Matsuki T, et al. TNF- α is crucial for the development of autoimmune arthritis in IL-1 receptor antagonist-deficient mice. *J Clin Invest* 2004;114:1603-11.
27. Dalum I, Jensen MR, Hindersson P, Elsner HI, Mouritsen S. Breaking of B cell tolerance toward a highly conserved self protein. *J Immunol* 1996;157:4796-804.
28. Dalum I, Jensen MR, Gregorius K, Thomasen CM, Elsner HI, Mouritsen S. Induction of cross-reactive antibodies against a self protein containing a foreign T helper epitope. *Mol Immunol* 1997;34:1113-20.
29. Dalum I, Butler DM, Jensen MR, Hindersson P, Steinaa L, Waterston AM, et al. Therapeutic antibodies elicited by immunization against TNF- α . *Nat Biotechnol* 1999;17:666-9.
30. Donnelly JJ, Ulmer JB, Liu MA. DNA vaccines. *Life Sci* 1997;60:163-72.
31. Youssef S, Wildbaum G, Maor G, Lanir N, Gour-Lavie A, Grabie N, et al. Long-lasting protective immunity to experimental autoimmune encephalomyelitis following vaccination with naked DNA encoding C-C chemokines. *J Immunol* 1998;161:3870-9.
32. Klinman DM, Currie D, Gursel I, Verthelyi D. Use of CpG oligodeoxynucleotides as immune adjuvants. *Immunol Rev* 2004; 99:201-16.
33. Hertz M, Mahalingam S, Dalum I, Klysner S, Mattes J, Neisig A, et al. Active vaccination against IL-5 bypasses immunological tolerance and ameliorates experimental asthma. *J Immunol* 2001; 167:3792-9.
34. Selby M, Goldbeck C, Pertile T, Walsh R, Ulmer J. Enhancement of DNA vaccine potency by electroporation in vivo. *J Biotechnol* 2000;83:147-52.